NASA

Technical Memorandum 83887

CLOUD TOP SCANNING RADIOMETER (CTS) USER'S GUIDE

K. S. Brown

NOVEMBER 1981

National Aeronautics and Space Administration

Goddard Space Flight Center
Greenbelt, Maryland 20771

CLOUD TOP SCANNING RADIOMETER (CTS)

USER'S GUIDE

K. S. Brown

November 1981

GODDARD SPACE FLIGHT CENTER
Greenbelt, Maryland

CLOUD TOP SCANNING RADIOMETER (CTS) USER'S GUIDE

K. S. Brown

ABSTRACT

The Cloud Top Scanning Radiometer (CTS) is an operational remote sensor that has collected data for meteorology studies. The CTS maps the earth's surface with a resolution of 0.1 km from an altitude of 18 km with 60 km side-to-side coverage of the field. It has three spectral channels. The 0.625 micrometer centered visual channel detects reflectance to within 1 percent. The 6.75 micrometer centered water vapor channel detects changes in temperature of less than one degree Kelvin at 175°K. The 11.5 micrometer centered infrared window channel detects changes of less one half degree Kelvin at 175°K. The data can be converted graphically into three display images of the scene. Values for scene temperature and albedo are calculated from calibration equations. The equations were derived from in-situ and laboratory measurements. Intercomparisons of the flight data temperatures with ground based and other remote sensor results established the certainty of the derived temperature values to within 3°K over a wide temperature range (180° to 320°K). The system performance, calibration, and operation have proved to be successful and the engineering information describing this system should prove useful to scientists and potential users of the data.

CONTENTS

LIST OF TABLES

LIST OF FIGURES

CLOUD TOP SCANNING RADIOMETER (CTS)
USER'S GUIDE

GENERAL

The Cloud Top Scanning Radiometer, (CTS), has been developed to collect spectral irradiance data in three wavelength bands. The bands, at 0.55 to 0.70 microns in channel 1, 6.5 to 7.0 microns in channel 2 and 10.5 to 12.5 microns in channel 3, determine solar albedo, atmospheric moisture temperature, and surface temperature respectively. The CTS spatially maps the ground with a resolution of approximately 0.1 km covering a 63 km wide field when flown from an aircraft platform at 18.7 km above the earth. The sequential mapping data, when graphically displayed, forms three images: one for each spectral channel. From the imagery spectral and spatial parameters such as cloud type, water content, temperature gradient, surface temperature, wind velocity, vertical velocity, frost and freeze, and cloud structure are determined.[1][2] Data users, normally the investigators and software specialists, require system specifications and response characteristic measurements to convert the raw flight data values into useful spectral and spatial information. The technical guide to convert the data for information extraction is contained in this user's manual. The user's manual also relates the information to engineering parameters and hardware system restrictions. Examples of CTS generated system restrictions due to the optics are illustrated and analytically treated. Expected output format values are specified so that flight anomalies can be detected. The engineering parameters needed for data analysis are detailed. And to make the user's guide a true reference for the scientist, it contains the calibration data for use in determining scene irradiance and blackbody temperature from the flight raw data.

SYSTEM PERFORMANCE

The CTS responds to spectral irradiance, detecting it with a sensitivity defined for the bandwidth of the channel. The energy band characterizes the input target. A brief description of the nature of each band is summarized as follows: channel 1 band: 0.55 to 0.70 microns. This reflective energy band partially includes the visual energy band and extends from 0.7 microns in the near infrared down in the visual to 0.5 microns. The sun is the primary daytime target scene source for this reflective or albedo measuring channel. Graphic display pictures of the target made from the channel 1 video data approximate a visual image. The image aids in visually determining cloud type and the albedo value is a measure of water content. The sensitivity of channel 1 was determined to be better than a change of 1 percent reflectivity over the range of 0.01 to 1.00 reflectivity. The other two spectral bands are in the infrared region of the spectra. The irradiance input in the bands is a function of temperature off the target from either the surface or the intrinsic atmospheric condition. The descriptions are as follows: channel 2: 6.5 to 7.0 microns. The infrared band at 6.5 to 7.0 microns is a water vapor absorption band detecting moisture in the optical layer of the atmosphere. The distance of layer penetration is approximately proportional to the location, amount, and temperature of the water vapor. Clouds at heights above the optical layer saturation distance (approximately 10 km) are normally detected while those below 10 km cannot be observed. The nominal output without cloud cover in the optical layer is usually a radiance proportional to the optical layer temperature; approximately 238 to 249 K. A visual image of this saturated atmosphere condition is a fairly constant color representing the saturated temperature (142 K) throughout the scene.

When high clouds are viewed, channel 2 detects their surface temperature and images the spatial structure surrounded by moisture contributions as associated with the optical layer. Sensitivity, the noise equivalent temperature difference (NETD) of channel 2, as measured in the lab, is better than 1 degree Kelvin at 185K. The range is 175K to 285K. Parenthetically, it is noted that the upper range temperature is only detectable under low moisture conditions or when viewing thru a short optical distance as for example, in the lab. Detecting sensitivity is given for the worse case condition since the rate of change of radiance increases with temperature. At 240K channel 2 discriminates a smaller NETD than at 175°K. The NETD is approximately 14 times better at 240K. The NETD of the instrument during flight is often degraded by a factor of two due to aircraft noise and data system conversion uncertainties.

Channel 3: 10.5 to 12.5 microns. The infrared band at 10.5 to 12.5 microns is an infrared window channel. Transmission thru the normal optical layer of atmosphere is almost one for this channel. This channel detects emitted radiance proportional to surface conditions of temperature and emittance. Basically images from this channel are spatial presentations of surface temperatures. Clouds are normally at lower temperature than ground surfaces and man-made features are normally at higher temperature than terrestrial ground surfaces. The channel 3 noise equivalent temperature difference (NETD) is better than 0.5K at 175K and the range is 175K to 330K. Sensitivity increases with temperature and becomes 6 times better at 273K. The NETD of the instrument during flight is often degraded by a factor of two due to aircraft noise and data system conversion uncertainties.

Additional performance features and a summary of sensitivity is shown in Table 1, CTS performance.[3] The type of detectors, optical and spectral characteristics and sensitivity are listed for each channel.

The main hardware assembly of the flight system is the sensor unit shown in Figure 1. The spatial mapping is performed by the scan mirror at 45° to the telescope axis. The mirror rotates in a plane perpendicular to the telescope axis, to scan the target below the sensor. A chopper between the telescope and relay optics modulates the incoming irradiance. The incomming modulated energy is divided into three paths by the relay dichroic filters and is focused on the three detectors. The output of each detector is a video signal.

IMAGERY

The CTS image system scan mechanism is basically the same type as used on many satellite scanning radiometers. A scan mirror rotates imaging a scan strip into the instantaneous field (IFOV) of the telescope. The strips, or scan lines are perpendicular to the aircraft flight line. Each strip is sequentially sampled at a fixed rate (the IFOV rate) starting from one edge of the scan line and continuing across the scene to the other edge. After viewing the trailing edge of the field the mirror continues rotating until it again lines up at the starting edge of the next strip and begins another line. During one revolution the aircraft has moved forward one IFOV and the consecutive scan lines contiguously map the scene. A display of many scan lines of data with each line as a display raster, results in an image of the scene.

A scene made up of scan lines 67km wide encompasses 120° total field of view under normal flight conditions. The scan period, based on an aircraft altitude of 18.4km, ground speed of 735kph (400kts) and 0.11km instantaneous field of view or 6.2mrad is 550ms. The maximum number of IFOV samples per scan period is 1012, but since the scene is viewed only for one

Table 1
CTS Performance

Parameter	Symbol	CH 1	CH 2	CH 3	Units
Detector-Area	A_d	0.05	0.05	0.05	cm^2
Noise Bandwidth	Δf_n	1012	1012	1012	Hz
Chopper Conversion Factor	α_{CH}	1.9	1.9	1.9	–
Electronic Noise Factor	α_e	1.7	1.7	1.7	–
Incremental Radiance with Temperature	$\left.\frac{\partial N}{\partial T}\right\rfloor_{185}$	–	1.58×10^{-7}	4.97×10^{-6}	$W/cm^2 - sr - K°$
Solid Angle	Ω	3.84×10^{-5}	3.84×10^{-5}	3.84×10^{-5}	sr
Entrance Aperture	A_o	324.3	324.3	324.3	cm^2
$D^*\Delta\lambda$	$D^*\Delta\lambda$	–	3.5×10^{10}	1.5×10^{10}	$cm - Hz^{1/2}/W$
Optical Efficiency	τ_0	0.13/0.16	0.41/0.44	0.28/0.39	–
Noise Equivalent Power	NEP	1.8×10^{-11}	–	–	$W/Hz^{1/2}$
Sensitivity Required	NEN (CH 1) NETD (2, 3)	0.32 (goal) $W/m^2 - sr$	1 K°	0.3 K°	–
Measured Sensitivity	NEN (1) NETD (2, 3)	0.32	0.81°K	0.3°K	–

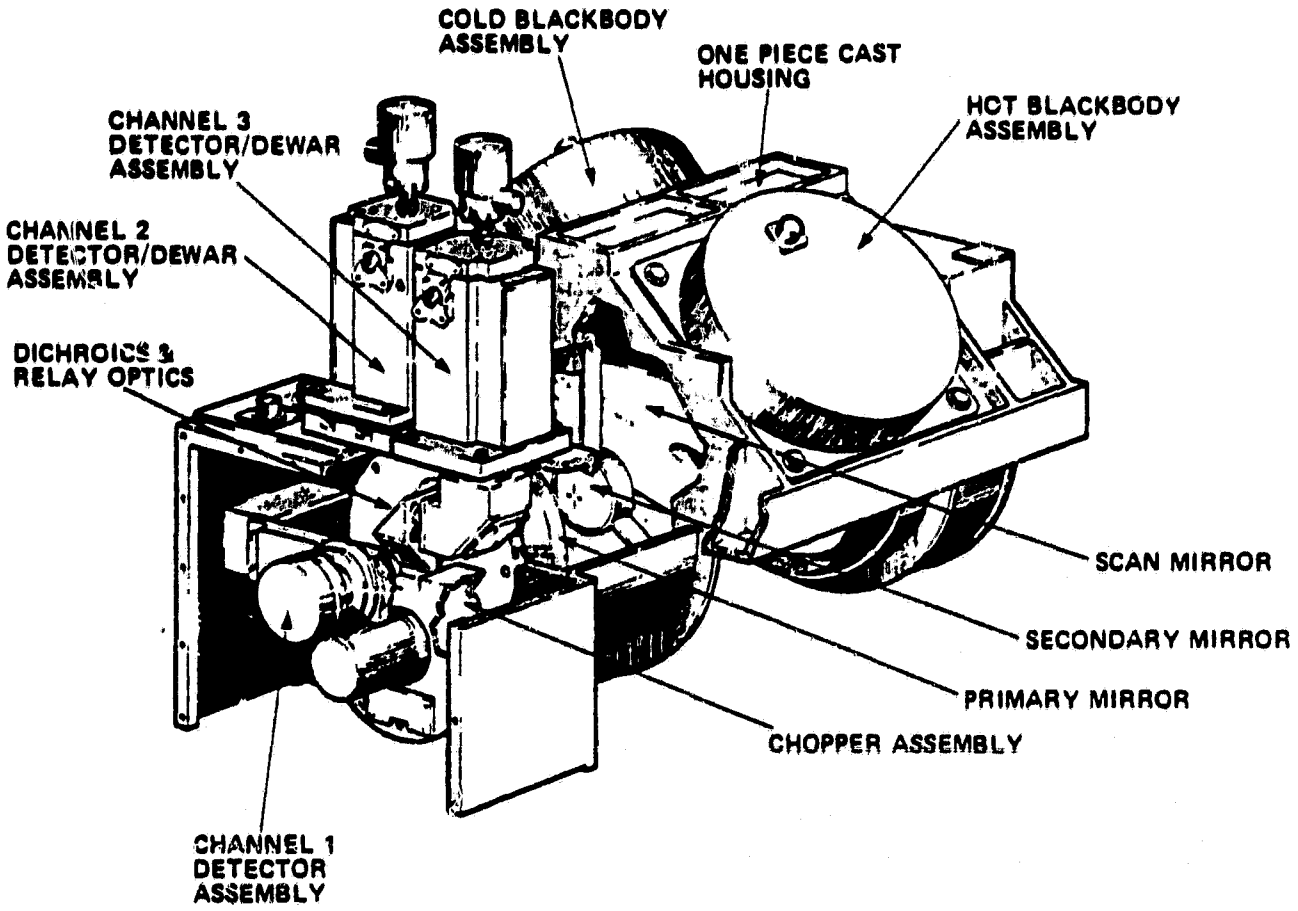

Figure 1. Cloud Top Scanning Radiometer Sensor Illustration

third of a revolution, the video data uses only 338. The other time spent in rotating the mirror around is called the backspan period. Each IFOV in the scene swath has a small distortion as the distance from the nadir increases.

The relationship is depicted geometrically in Figure 2.[4] The length of the IFOV footprint, s, is smallest at nadir and varies with angle as follows:

$$s \simeq \frac{h\alpha}{\cos^2\theta} \text{ [km]}$$

where s = length of IFOV, km; α = IFOV angle, radians
h = altitude, km; θ = nadir angle, radians

The sides increase and rotate from the square shape because of the scan mirror 45° and off axis combined tilt. Actually the shape of the IFOV footprint changes with angle also. It becomes a rhombus with non equal adjacent sides. The approximate IFOV footprint size change is given in the curve of Figure 3. Note that the IFOV increases to eight times the size of the nadir IFOV. These variations due to the aircraft-to-ground geometry are usually referred to in texts as the "Bow Tie Scan".[5]

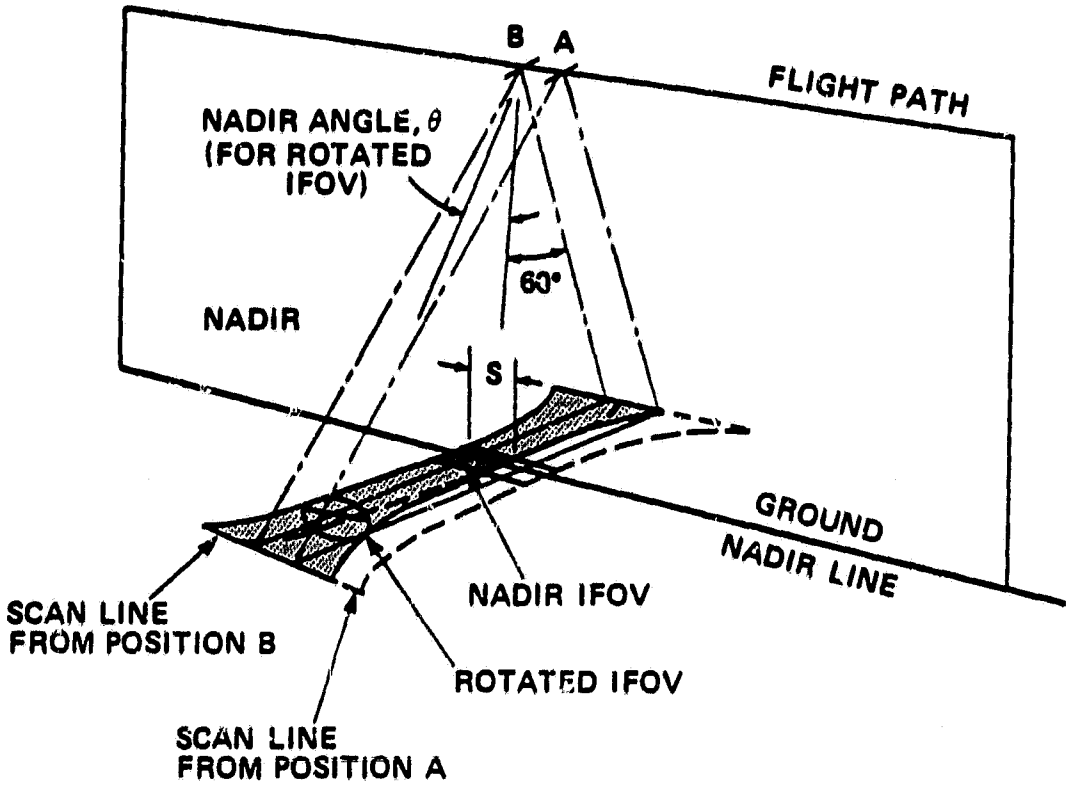

Figure 2. Scan Line and IFOV Geometric Illustration

There are also IFOV sample changes due to cloud height above the surface of the ground. The IFOV footprint is a function of the distance from the scanner to the cloud surface. It becomes smaller as the cloud, altitude increases. The change results in undersampling of the cloud. The relation of sample area, A, as a function of cloud height is:

$$A = \frac{(0.1 - 0.0062h)\,(0.1)}{\cos^4\theta} \quad [km^2]$$

where A = IFOV area, km^2
h = cloud altitude, km
θ = nadir angle, radians

The cloud sample reduces to the ground IFOV footprint sample when h is zero. A three dimensional view of a surface simulating a cloud under the nadir halfway between ground and the aircraft is given in Figure 4. The skipping of the scan lines or undersampling is shown in the IFOV traces in the top view. Since IFOV rate is invarient, along the scan line the number of IFOV's is unchanged in this direction. This results in an unusual image distortion. The true scale length remains fixed in the direction of travel but the scan length at altitude due to the fixed angular representation changes with altitude. The front view of the figure shows the relation between a

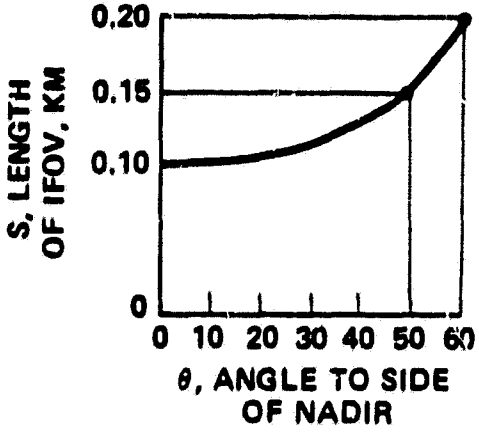

Figure 3. Change in Scan Line IFOV

high altitude dimension and surface dimension. A feature centered under nadir has a dimension along the scan proportional to the cloud height as follows:

$$L_t = L_s \frac{(h_a - h_c)}{h_a} \text{ [km]}$$

where L_t = true dimension, km
L_s = image dimension along scan line, km
h_a = aircraft altitude, km
h_c = cloud altitude, km

This relation between cloud height and the ratio of CTS imagery to photo coverage dimensions can be used to geometrically determine the approximate cloud height. In cases where the domes are identified as being circular, all that is required is measuring the length along the flight line and across the flight line in the CTS imagery and computing altitude from the above equation. The photography which tends to show true shape can be checked to verify the true shape. A CTS image of a circular shape such as a dome will be elliptical with the major axis along the cross track axis. Changing the image swath in the display can compensate for this distortion.

The sampling of clouds at high altitude can alias gradients in the flight direction. This is due to undersampling. Those temperatures along nadir will tend to differ from gradients in the scan direction. Samples of the sides of clouds can also alias data resulting in three dimensional effects on data normally assumed to be at one height. The aliasing may be of importance to the scientists. The equations and image description can be of help in determining the nature of the temperature, sampling, and three dimension contributions in a set of data.

DATA FORMAT

The scan period is dependent upon aircraft altitude, h, and telescope system IFOV angle, α, as expressed in the following equation:

$$s = \frac{h\alpha}{v} \text{ [sec]}$$

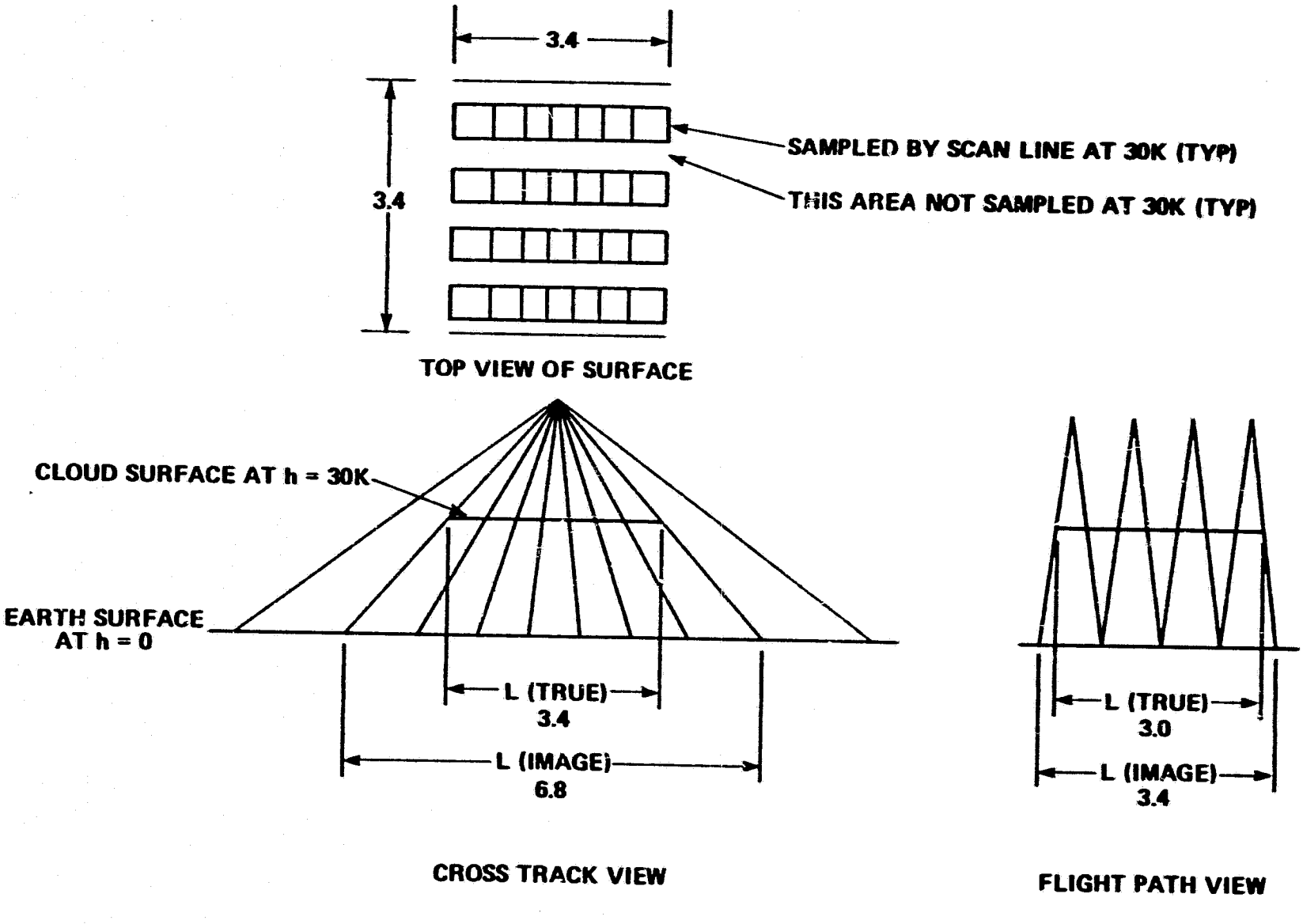

Figure 4. Sampling and Image Length Relationships

where s = scan period, sec
h = altitude, km
α = IFOV angle, radians
v = Aircraft speed, km/sec

The CTS scan period calculated for nominal operation with contiguous scanning of the ground is 550 ms at the nominal RB-57 flight altitude and speed. The scene data is collected along a swath whose included angle is ±60° off the aircraft nadir. This included angular total field, at nominal height is equivalent to a 63 km swath at the 18.7 altitude. The collection of scene data as the mirror turns thru the swath is called the video data event. When the mirror passes the trailing edge of the swath it keeps rotating until it lines up again at the edge of next swath. During the interval when the mirror travels from the end of one swath to the start of the next one, video data is not being collected. This backscan period is available for multiplexing engineering data onto the channel output in a systematic format. This data format is listed in Table 2. The time and mirror angle are for reference to the scan period and one complete revolution respectively. The column marked event lists the abbreviation which is used in the data software and printouts. The raw counts are digitized values of the CTS analog voltages as normally recorded in flight. A discussion of the purpose of the format events is as follows:

1. Scene Video

Detector outputs of the swath data from the scene which are collected by a channel. Actually three tables of output format are condensed into this one table. The three outputs differ as noted in the column headed raw counts and volts.

2. IV0, IV1, IV2, IV3, IV4, IV5

Electronic engineering voltages multiplexed onto the output which establish the relation between the analog signal voltage and digitized values for the signal. The computer program uses linear regression analysis to determine the relationship between the voltage, which was measured in the lab, and the raw counts.

3. IHBB1, IHBB2, IHBB3

The three precision resistance thermocouples mounted on the hot blackbody target that measure its temperature. These electronic generated voltages are multiplexed onto the output to be used in calculating the irradiance of the hot blackbody.

4. ICBB, ICBB2, ICBB3

The three precision resistance thermocouples mounted on the cold blackbody target that measure its temperature. These electronics generated engineering voltages are multiplexed onto the output to be used in calculating irradiance of the cold blackbody.

5. ITHRM1, ITHRM2, ITHRM3

Three temperature thermistor mounted on the sensor to monitor temperature in flight. The electronics generated engineering voltages are multiplexed onto the output for checking the sensor environment temperature.

6. IVB1

An electronics null output used to space events for timing purposes.

Table 2
Format

Time MS	Mirror Angle	Event	Description	Raw Counts	Voltage	IFOV Samples
0-184	0-120	Scene Video	Detector Output Scan Line Swath of Target	(Different in Each Channel)		338
.189	123.6	IV0	Electronics Generated Zero Volt Calibration Level	5-9	0	10
.195	127.2	IV1	Electronics Generated One Volt Calibration Level	98-104	1.00	10
.200	130.8	IV2	Electronics Generated Two Volt Calibration Level	197-202	2.00	10
.206	134.4	IV3	Electronics Generated Three Volt Calibration Level	295-300	3.00	10
.211	138.0	IV4	Electronics Generated Four Volt Calibration Level	386-400	4.00	10
.217	141.6	IV5	Electronics Generated Five Volt Calibration Level	482-500	5.00	10
.222 .228 .223	145.2 148.8 152.4	IHBB1 IHBB2 IHBB3	Electronics Generated Hot Blackbody Thermocouples Three Units on the Hot Blackbody Target	400-500 400-500 400-500	4-5 4-5 4-5	10 10 10
.239 .244 .250	156.0 159.6 163.2	ICBB1 ICBB2 ICBB3	Electronics Generated Cold Blackbody Thermocouples Three Units on the Cold Blackbody Target	80-180 80-180 80-180	0.8-1.8 0.8-1.8 0.8-1.8	10 10 10
.255 .261 .266	166.8 170.4 174.0	ITHRM1 ITHRM2 ITHRM3	Electronics Generated Thermistors on the Telescope, Chopper, and Relay Optics	150-180 160-190 170-200	1.5-1.8 1.6-1.9 1.7-2.0	10 10 10
.288	185.0	IVB1	Electronics Zero	4-9	0.05	31
.289	189.0	ICCPUL	Electronics Pulse	505-511	5.1	11
.308	201.0	ICCVID	Detector Generated Cold Blackbody Video	(Different in Each Channel)		34
.352	230.0	IVB2	Electronics Zero	4-9	0.05	82
.358	234.0	IVCPUL	Electronics Pulse	505-511	5.1	11
.376	246.0	IVCVID	Detector Generated Visible Channel Zero	(Different in Each Channel)		34
.421	275.0	IVB3	Electronics Zero	4-9	0.05	82
.429	279.0	IHCPUL	Electronics Pulse	505-511	5.1	11
.445	291.0	IHCVID	Detector Generated Hot Blackbody Video	(Different in Each Channel)		34
.545	356.0	IVB4	Electronics Zero	4.9	0.05	184
.551	360.0	ISSPUL	Electronics Pulse	505-511	5.1	11

7. ICCPUL

An electronics pulse used to flag an upcoming video event, in this case the collection of the cold calibration video data.

8. ICCVID

A detector generated voltage output proportional to the irradiance calculated from the cold blackbody precision resistance thermocouples. Channels 2 and 3 respond to this cold target output, Channel 1 is zero.

9. IVB2

Same function as IVB1.

10. IVCPUL

An electronic pulse flagging an upcoming video event, in this case the collection of the Channel 1 dark voltage calibration level.

11. IVCVID

A detector generated video voltage output used to determine the C l dark voltage level. Channels 2 and 3 are both generating an output also. Their output ent the radiance off the dark video target. Since the target is between the hot and cold ckbodies, this is a radiance proportional to a composite temperature of the blackbodies and walls of the housing.

12. IVB3

Same function as IVB1.

13. IHCPUL

An electronics pulse flagging an upcoming video event, the hot blackbody detector generated voltage proportional to the hot blackbody temperature.

14. IHBBVID

The detector generated video voltage output proportional to the hot blackbody target irradiance.

15. IVB4

Same function as IVB1.

16. ISSPUL

The electronic generated pulse flagging the upcoming video event described previously as scene video.

The events described are repeated each mirror rotation as scene data is collected. The repeating format is useful in determining the operating performance of the instrument. If the events repeat. then it is likely the electronics is operational. If the detector video blackbody and zero level

repeat it is likely that for a given detector channel, the video data is operating nominally. By counting the number of IFOV data words the exact timing can be determined. For a 10 minute collection of data over the target, 1091 scan lines are collected. During this time the aircraft travels approximately 109km. This distance can be a function of true airspeed checked with the ground coordinates. It is usually necessary for the user to coordinate the output with ground features, coordinates, time, and altitude. The relation of the output to the aircraft ground path and the preservation of system location is described briefly in the next section.

CTS SYSTEM RAW DATA FORM

Generally the CTS output is a repeating format (as previously described) without reference to the actual mission and coordinates for location. The important aircraft flight record of the day, time of day, number of each individual scan line, and channel are added to the CTS output. The aircraft timing and flight autopilot data are recorded as separate information. The telemetry system originates and inserts time and scan number identification in front of each scan line. The two records, the aircraft flight location tape, and the CTS flight data tape are merged on a computer producing a scientific raw data tape that has a header detailing the general mission parameters. On this tape which is usually one set of target scene passes (seldom exceeding 2500 scan lines) each scan line is followed by timing and aircraft location data corresponding to scan location. This merged tape is used for extracting data. The user can determine the exact time and relate position to ground features or bench mark cloud scenes by reading trailer data.

An intermediate step in the processing of data which can become important if difficulties arise is the rerecording on the ground of flight tape. The need for this conversion arises because the flight data is recorded serially and the ground Atmospheric Oceanographic Information Process System (AOIPS) reads tape in a parallel byte sequence. The incompatibility between flight serial and computer parallel taping is related to flight recorder performance and the high density packing of data needed during unattended operation on board the aircraft.

The data in the merged parallel form described as the user tape can be processed on the AOIPS system or listed. The listing can include trailer information and all CTS format engineering data as well as the scene video data.

CHANNEL 1 CALIBRATION

Calibration in channel 1 is performed with the set-up shown schematically in Figure 5. The input source is a diffuse target case consisting of a 6 foot integrating sphere with lamps internally mounted which can be operated in sequence to produce up to 12 levels of intensity. The CTS is positioned so that the source geometrically fills the aperture, this near field set-up reduces the response view angle and area variability.[6] A ground station samples the format output at the scene video, the dark video voltage, and the electronics generated reference voltage events and records the data. Thirty voltage samples are statistically averaged to determine the response at each lamp level. The response curve is determined as the regression of the voltage versus input irradiance level: The curve is shown in Figure 6.

The relative spectral response for channel 1,[7] a function of the system optics, filters and detectors is listed in Table 3.

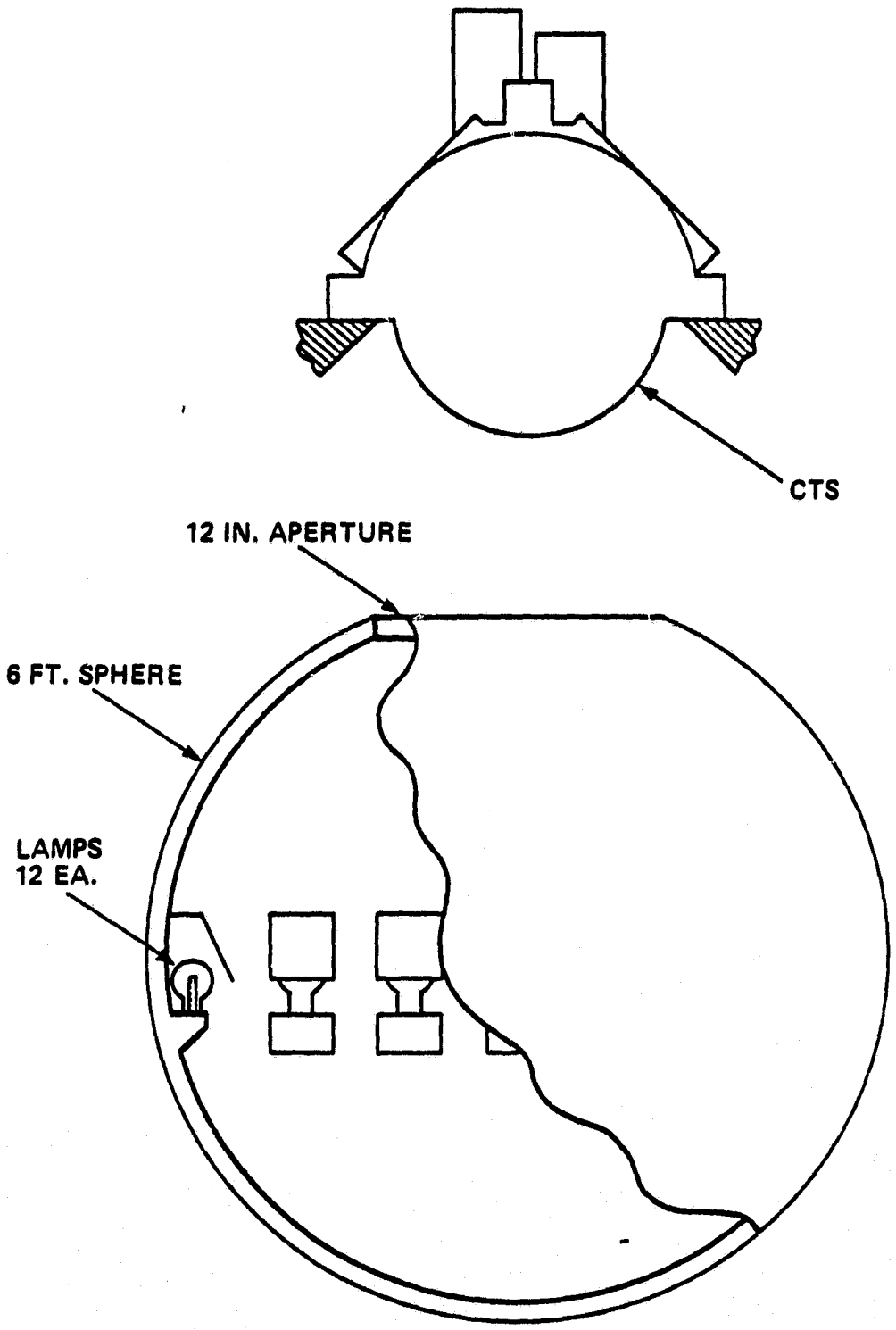

Figure 5. Channel 1 Calibration Set-up

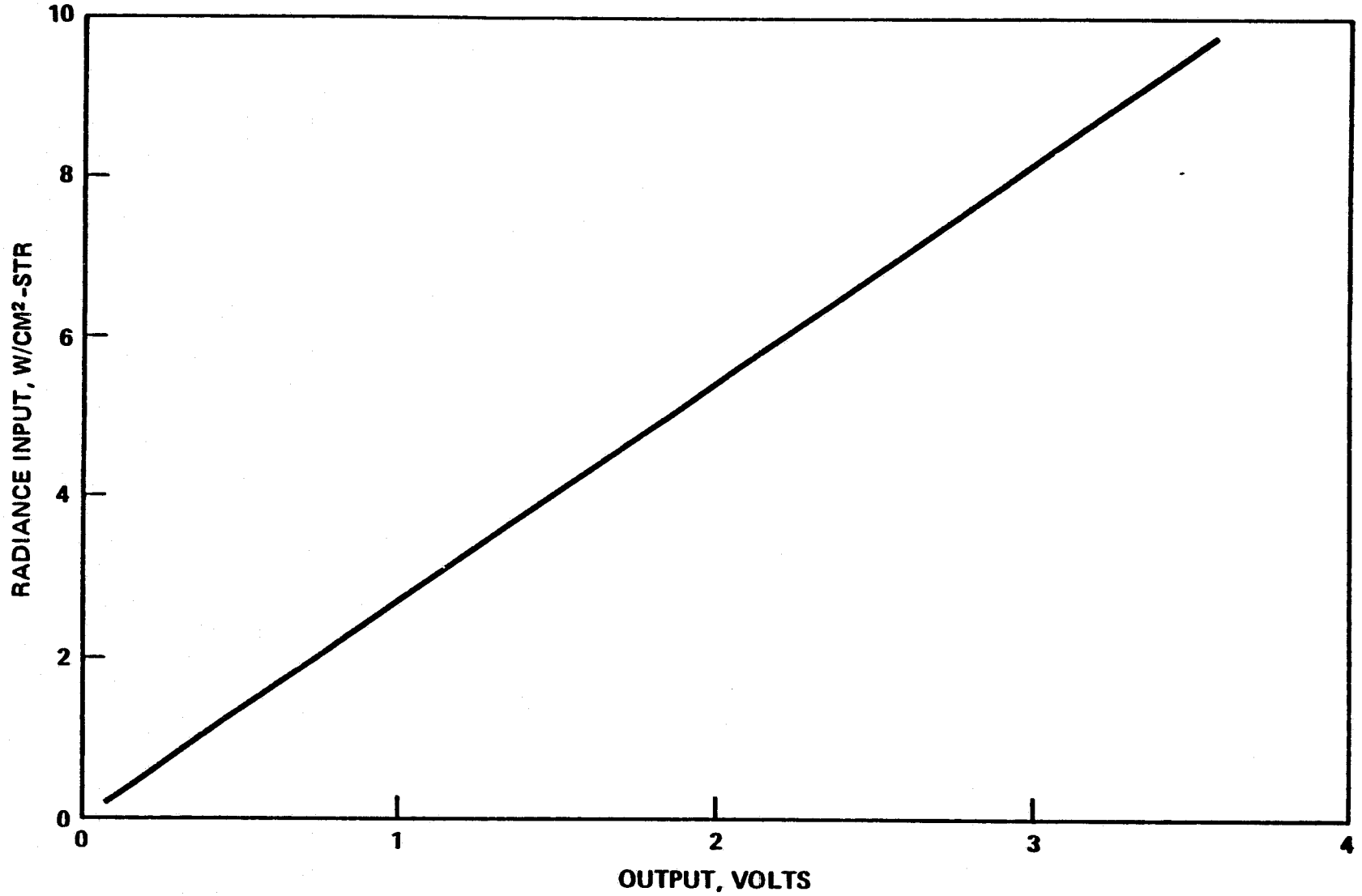

Figure 6. Channel 1 Calibration Curve

Table 3
Channel 1 Relative Spectral Response

Response Normalized	Wavelength Microns	Response Normalized	Wavelength Microns
0.000	0.525	0.9465	0.665
0.02984	0.530	0.9136	0.670
0.09979	0.535	0.8786	0.675
0.1934	0.540	0.8657	0.680
0.02809	0.545	0.8251	0.685
0.3611	0.550	0.8200	0.690
0.4527	0.555	0.8313	0.695
0.5700	0.560	0.8642	0.700
0.7150	0.565	0.9356	0.705
0.8560	0.570	0.9743	0.710
0.9475	0.575	0.9949	0.715
0.9671	0.580	0.9156	0.720
0.9465	0.585	0.7263	0.725
0.9167	0.590	0.5051	0.730
0.9064	0.595	0.3292	0.735
0.9126	0.600	0.2119	0.740
0.9311	0.605	0.1379	0.745
0.9434	0.610	0.0947	0.750
0.9486	0.615	0.0669	0.755
0.9465	0.620	0.0494	0.760
0.9414	0.625	0.0370	0.765
0.9403	0.630	0.03086	0.770
0.9465	0.635	0.02572	0.775
0.9588	0.640	0.02366	0.780
0.9784	0.645	0.02160	0.785
0.9907	0.650	0.0000	0.790
0.9928	0.655	0.0000	0.795
0.9774	0.660		

CHANNEL 2 CALIBRATION

The set-up for calibration of channel 2 is shown schematically in Figure 7. The source is an infrared target whose emissive coefficient approaches unity. The surface of this blackbody source is a honeycomb which geometrically increases the absorptivity. The target temperature is monitored by several precision resistance thermocouples. The temperature of the source, thermal gradient, and stability are dynamically controlled. The target completely fills the aperture of the CTS. This is a near field set-up to reduce the angular and area dependency of the CTS system. The background input is reduced by cooling the chamber to liquid nitrogen temperature. The instrument temperature is externally controlled and monitored. Coils conduct heat to the CTS to keep it at a constant temperature selected to approximate the flight operating temperature.

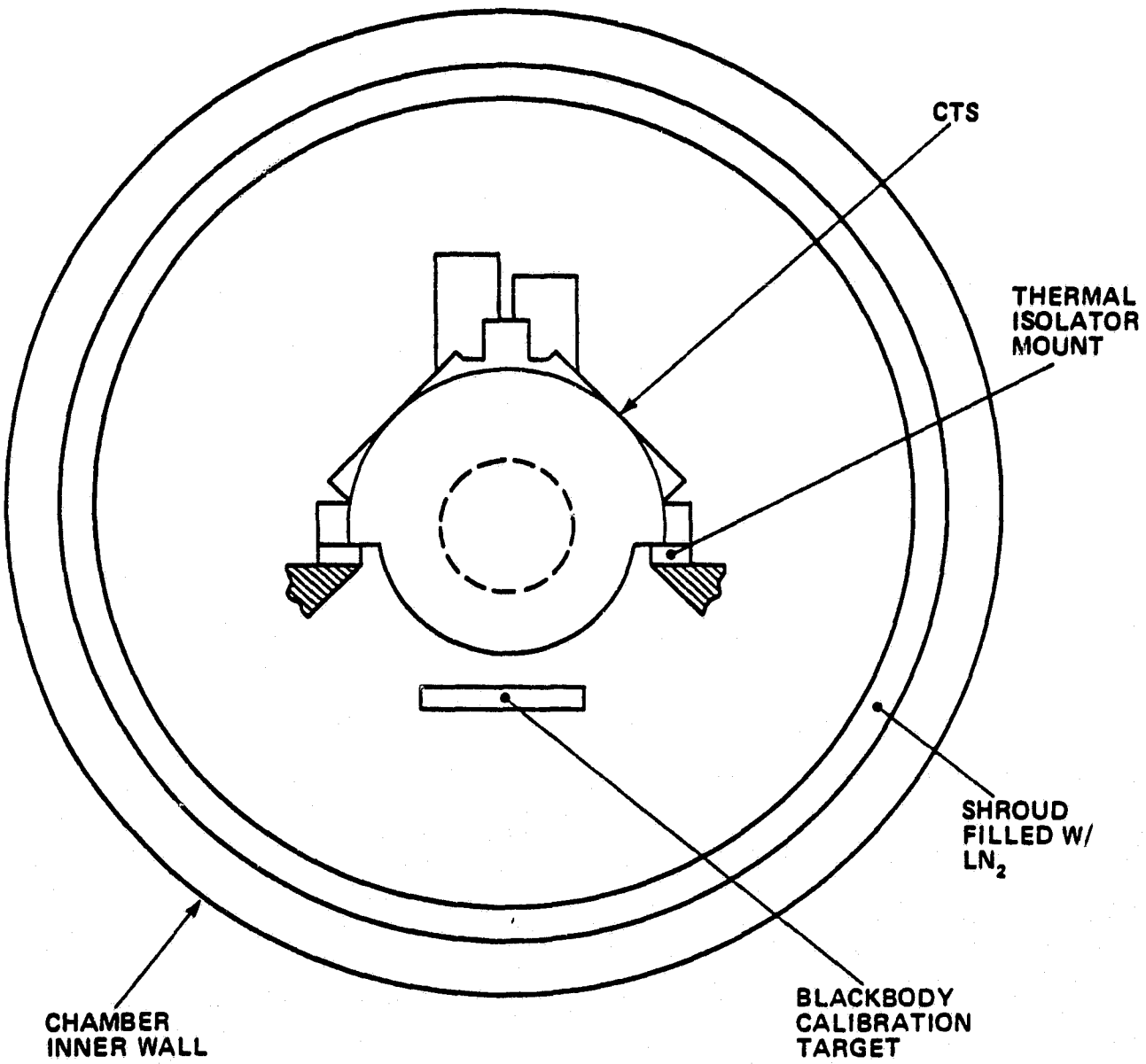

Figure 7. Channel 2 Calibration Set-up Schematic

The scene video voltage of channel 2 and the blackbody temperature are measured and recorded. The blackbody output is incrementally changed to record data at various input irradiance levels. The resulting curve of blackbody irradiance input vs. output video voltage is shown in Figure 8.

The spectral response of the system was measured. The irradiance at a given temperature was calculated using Plank's equation and the convoluted spectral transmission. Table 4 lists the irradiance at the incremental calculated temperatures.

CHANNEL 3 CALIBRATION

The set-up for calibration of channel 3 and taking of data was performed identically to channel 2. The responsivity results are plotted in Figure 9. The irradiance versus temperature spectral response calculations are listed in Table 5.

IN-SITU TARGET CALIBRATION

The output of each internal target is calibrated with respect to the average of the three internal precision resistance thermocouples. This calibration is performed identical to the infrared calibration for the detectors. The average voltage of the three thermocouples is measured when the detector voltage for the scene video is equal to the voltage for the instrument blackbody video. Shown graphed in Figure 10 is the curve of the cold blackbody temperature versus cold blackbody thermocouple voltage. The curve in Figure 11 relates the hot blackbody temperature to the hot blackbody thermocouple voltage.

CHECK FOR IN-SITU TEMPERATURE OFFSET

The internal blackbodies provide two points of detector voltage response to known input irradiance. This information is used to correct the offset of the second order equation. A graph of the check data superimposed on a response curve is shown in Figure 12. The calculated offset is labeled and also shown is the adjustment to the equation. This procedure is used in the calibration program for determining temperatures.

CLOSURE

The CTS has been flown over surface and cloud targets. Its thermal calibration on cold scenes has been verified by radiosonde ground truth and lidar intercomparison for conversion of height to temperature. The channel 3 temperature variability with respect to lidar cloud height is approximately 1-1/2-3° at 200°K for the September 23, 1979 flight. The sea surface was used to check the high temperatures variability. The temperature recorded by the CTS over a Florida bay was 288°K. The estimated temperature was 300°K. The difference is partly due to the optical layer temperature, which was not calculated. Estimates of a 3 to 4° low reading difference are apparently due to the uncertainty in the sensor calibration at this end of the response range. Scene images have been observed and appear nominal for the scan system. No data drop outs or failures have occurred during the June and September flights. The calibration data is updated for each flight and it is advisable for users to obtain the latest calibration information from the programming source for the data set being investigated.

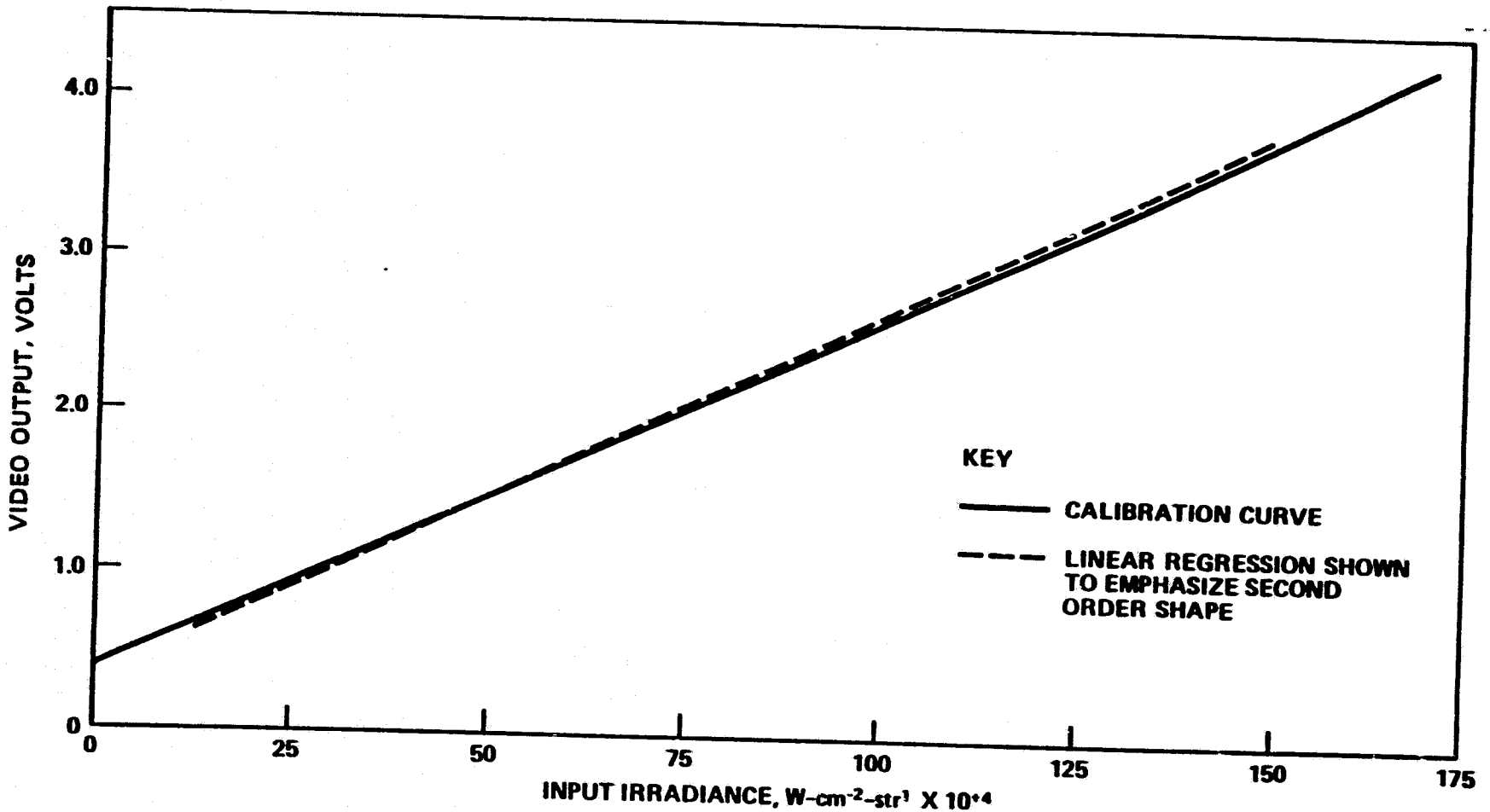

Figure 8. Channel 2 Irradiance Response Calibration Curve

Table 4
Channel 2 System Temperature Response

Temp °K	Radiance W/cm² – STR	Temp °K	Radiance W/cm² – STR	Temp °K	Radiance W/cm² – STR	Temp °K	Radiance W/cm² – STR	Temp °K	Radiance W/cm² – STR	Temp °K	Radiance W/cm² – STR
175	1.90165E-6	195	6.63342E-6	215	1.83525E-5	235	4.27211E-5	255	8.71361E-5	275	1.60277E-4
176	2.03788E-6	196	7.01407E-6	216	1.92155E-5	236	4.43978E-5	256	9.00348E-5	276	1.64855E-4
177	2.18217E-6	197	7.41238E-6	217	2.01105E-5	237	4.61255E-5	257	9.30063E-5	277	1.69529E-4
178	2.33489E-6	198	7.82896E-6	218	2.10385E-5	238	4.79050E-5	258	9.60518E-5	278	1.74301E-4
179	2.49642E-6	199	8.26442E-6	219	2.20003E-5	239	4.97375E-5	259	9.91724E-5	279	1.79172E-4
180	2.66715E-6	200	8.71939E-6	220	2.29967E-5	240	5.16240E-5	260	1.02369E-4	280	1.84142E-4
181	2.84747E-6	201	9.19453E-6	221	2.40287E-5	241	5.35656E-5	261	1.05644E-4	281	1.89214E-4
182	3.03781E-6	202	9.69048E-6	222	2.50971E-5	242	5.55633E-5	262	1.08997E-4	282	1.94388E-4
183	3.23859E-6	203	1.02079E-5	223	2.62028E-5	243	5.76181E-5	263	1.12430E-4	283	1.99666E-4
184	3.45025E-6	204	1.07475E-5	224	2.73467E-5	244	5.97313E-5	264	1.15943E-4	284	2.05049E-4
185	3.67324E-6	205	1.13100E-5	225	2.85297E-5	245	6.19037E-5	265	1.19539E-4	285	2.10537E-4
186	3.90801E-6	206	1.18960E-5	226	2.97528E-5	246	6.41367E-5	266	1.23218E-4		
187	4.15504E-6	207	1.25063E-5	227	3.10169E-5	247	6.64311E-5	267	1.26982E-4		
188	4.41482E-6	208	1.31416E-5	228	3.23229E-5	248	6.87883E-5	268	1.30862E-4		
189	4.68784E-6	209	1.38026E-5	229	3.36718E-5	249	7.12091E-5	269	1.34768E-4		
190	4.97461E-6	210	1.44901E-5	230	3.50646E-5	250	7.36949E-5	270	1.38792E-4		
191	5.27566E-6	211	1.52049E-5	231	3.65023E-5	251	7.62466E-5	271	1.42906E-4		
192	5.59151E-6	212	1.59478E-5	232	3.79858E-5	252	7.88655E-5	272	1.47110E-4		
193	5.92271E-6	213	1.67195E-5	233	3.95160E-5	253	8.15526E-5	273	1.51406E-4		
194	6.26982E-6	214	1.75208E-5	234	4.10941E-5	254	8.43091E-5	274	1.55794E-4		

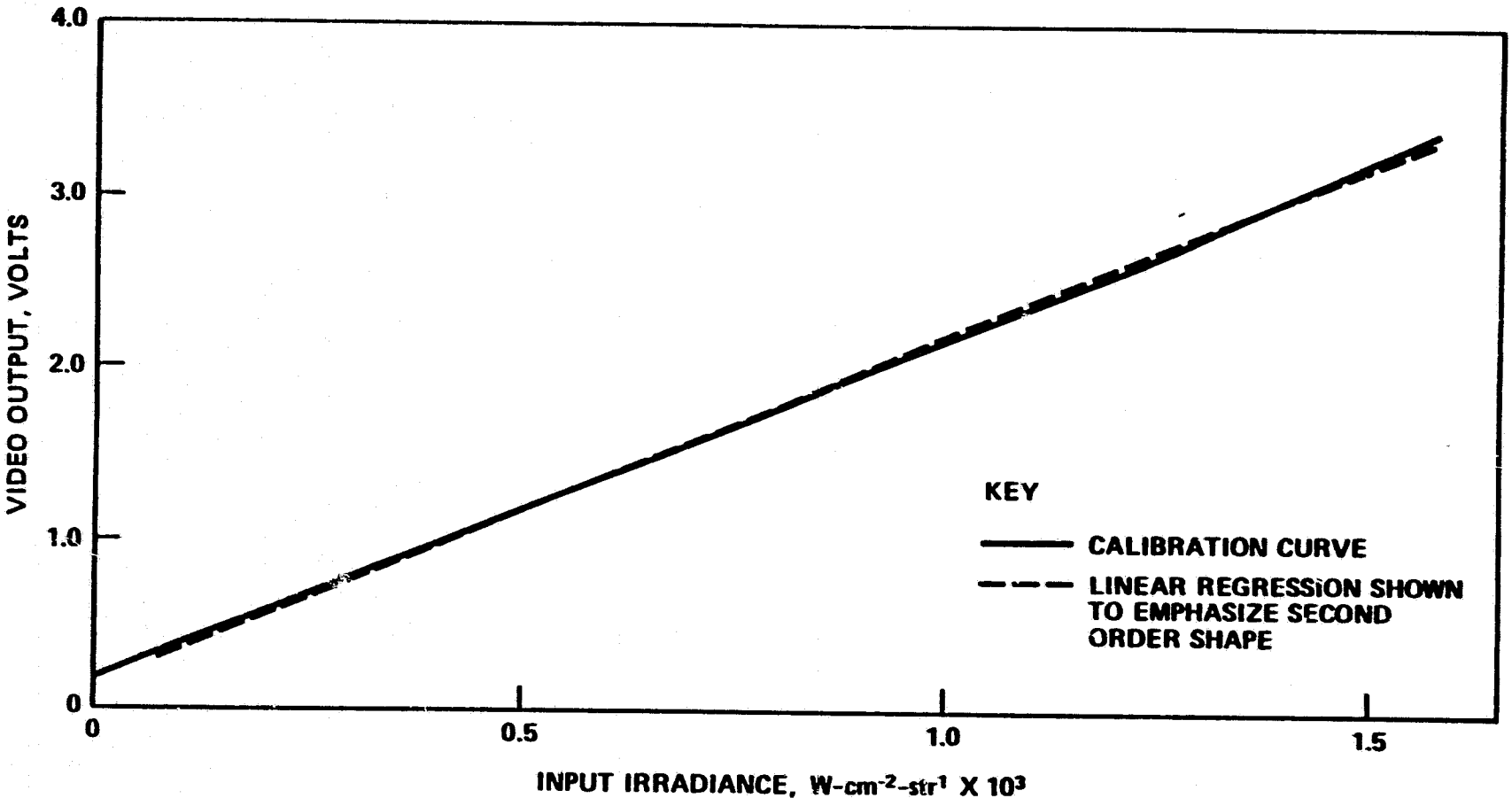

Figure 9. Channel 3 Irradiance Response Calibration Curve

Table 5
Channel 3 System Temperature Response

Temp °K	Radiance W/cm² – STR	Temp °K	Radiance W/cm² – STR	Temp °K	Radiance W/cm² – STR	Temp °K	Radiance W/cm² – STR	Temp °K	Radiance W/cm² – STR	Temp °K	Radiance W/cm² – STR
182	9.37758E-5	207	2.17955E-4	232	4.23367E-4	257	7.24249E-4	282	1.12875E-3	307	1.63980E-3
183	9.74177E-5	208	2.24497E-4	233	4.33496E-4	258	7.38405E-4	283	1.14715E-3	308	1.66245E-3
184	1.01160E-4	209	2.31171E-4	234	4.43779E-4	259	7.52727E-4	284	1.16571E-3	309	1.68528E-3
185	1.05003E-4	210	2.37978E-4	235	4.54217E-4	260	7.67217E-4	285	1.18444E-3	310	1.70827E-3
186	1.08949E-4	211	2.44918E-4	236	4.64811E-4	261	7.81874E-4	286	1.20335E-3	311	1.73143E-3
187	1.13000E-4	212	2.51994E-4	237	4.75561E-4	262	7.96699E-4	287	1.22243E-3	312	1.75476E-3
188	1.17156E-4	213	2.59206E-4	238	4.86467E-4	263	8.11692E-4	288	1.24167E-3	313	1.77825E-3
189	1.21419E-4	214	2.66555E-4	239	4.97532E-4	264	8.26853E-4	289	1.26109E-3	314	1.80192E-3
190	1.25791E-4	215	2.74043E-4	240	5.08754E-4	265	8.42183E-4	290	1.28068E-3	315	1.82575E-3
191	1.30272E-4	216	2.81669E-4	241	5.20135E-4	266	8.57681E-4	291	1.30044E-3	316	1.84975E-3
192	1.34864E-4	217	2.89436E-4	242	5.31676E-4	267	8.73349E-4	292	1.32037E-3	317	1.87392E-3
193	1.39569E-4	218	2.97343E-4	243	5.43377E-4	268	8.89186E-4	293	1.34047E-3	318	1.89825E-3
194	1.44388E-4	219	3.05393E-4	244	5.55237E-4	269	9.05192E-4	294	1.36075E-3	319	1.92276E-3
195	1.49321E-4	220	3.13586E-4	245	5.67259E-4	270	9.21367E-4	295	1.38119E-3	320	1.94742E-3
196	1.54371E-4	221	3.21922E-4	246	5.79443E-4	271	9.37713E-4	296	1.40181E-3	321	1.97226E-3
197	1.59539E-4	222	3.30404E-4	247	5.91788E-4	272	9.54228E-4	297	1.42259E-3	322	1.99726E-3
198	1.64825E-4	223	3.39031E-4	248	6.04296E-4	273	9.70913E-4	298	1.44355E-3	323	2.02243E-3
199	1.70232E-4	224	3.47805E-4	249	6.16966E-4	274	9.87769E-4	299	1.46467E-3	324	2.04776E-3
200	1.75760E-4	225	3.56726E-4	250	6.29801E-4	275	1.00479E-3	300	1.48597E-3	325	2.07326E-3
201	1.81411E-4	226	3.65795E-4	251	6.42798E-4	276	1.02199E-3	301	1.50743E-3	326	2.09892E-3
202	1.87185E-4	227	3.75013E-4	252	6.55961E-4	277	1.03936E-3	302	1.52907E-3	327	2.12475E-3
203	1.93084E-4	228	3.84381E-4	253	6.69287E-4	278	1.05690E-3	303	1.55088E-3	328	2.15074E-3
204	1.99110E-4	229	3.93900E-4	254	6.82779E-4	279	1.07460E-3	304	1.57285E-3	329	2.17689E-3
205	2.05263E-4	230	4.03570E-4	255	6.96437E-4	280	1.09248E-3	305	1.59500E-3		
206	2.11544E-4	231	4.13402E-4	256	7.10260E-4	281	1.11053E-3	306	1.61731E-3		

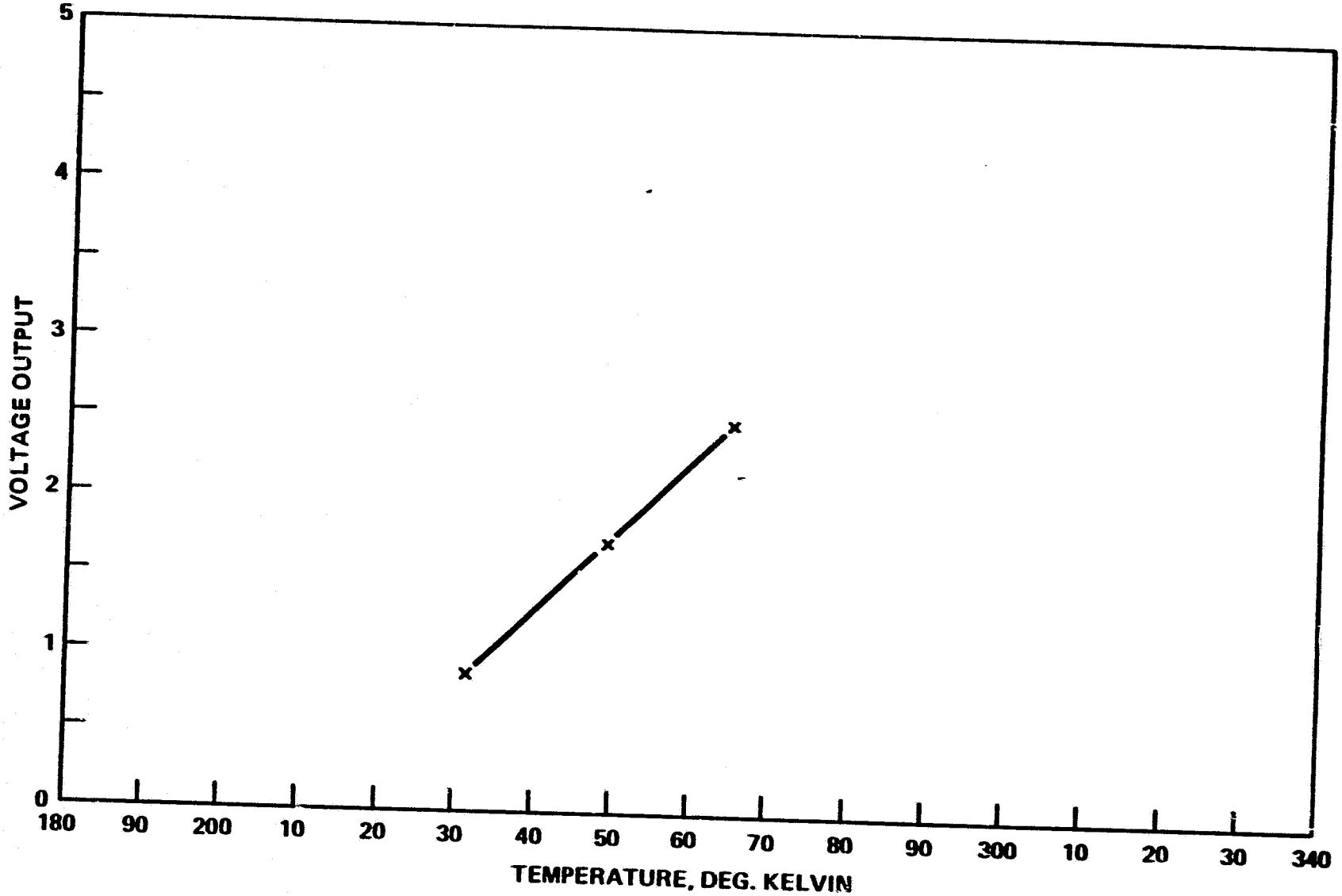

Figure 10. Cold Blackbody Thermistor Calibration, T = 20.83496922 V + 212.9353338

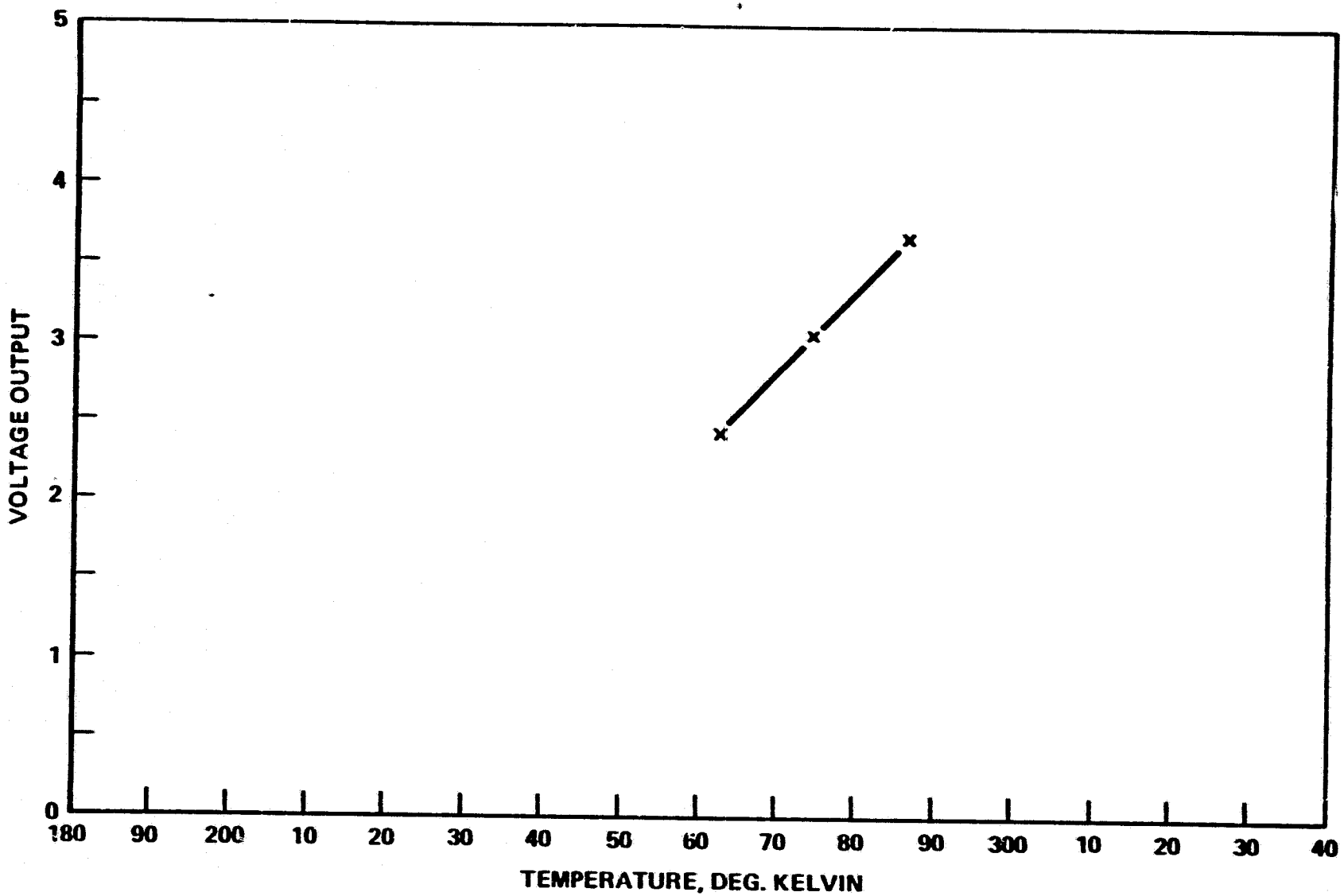

Figure 11. Hot Blackbody Thermistor Calibration, T = 215.2570476 + 19.28918216 V

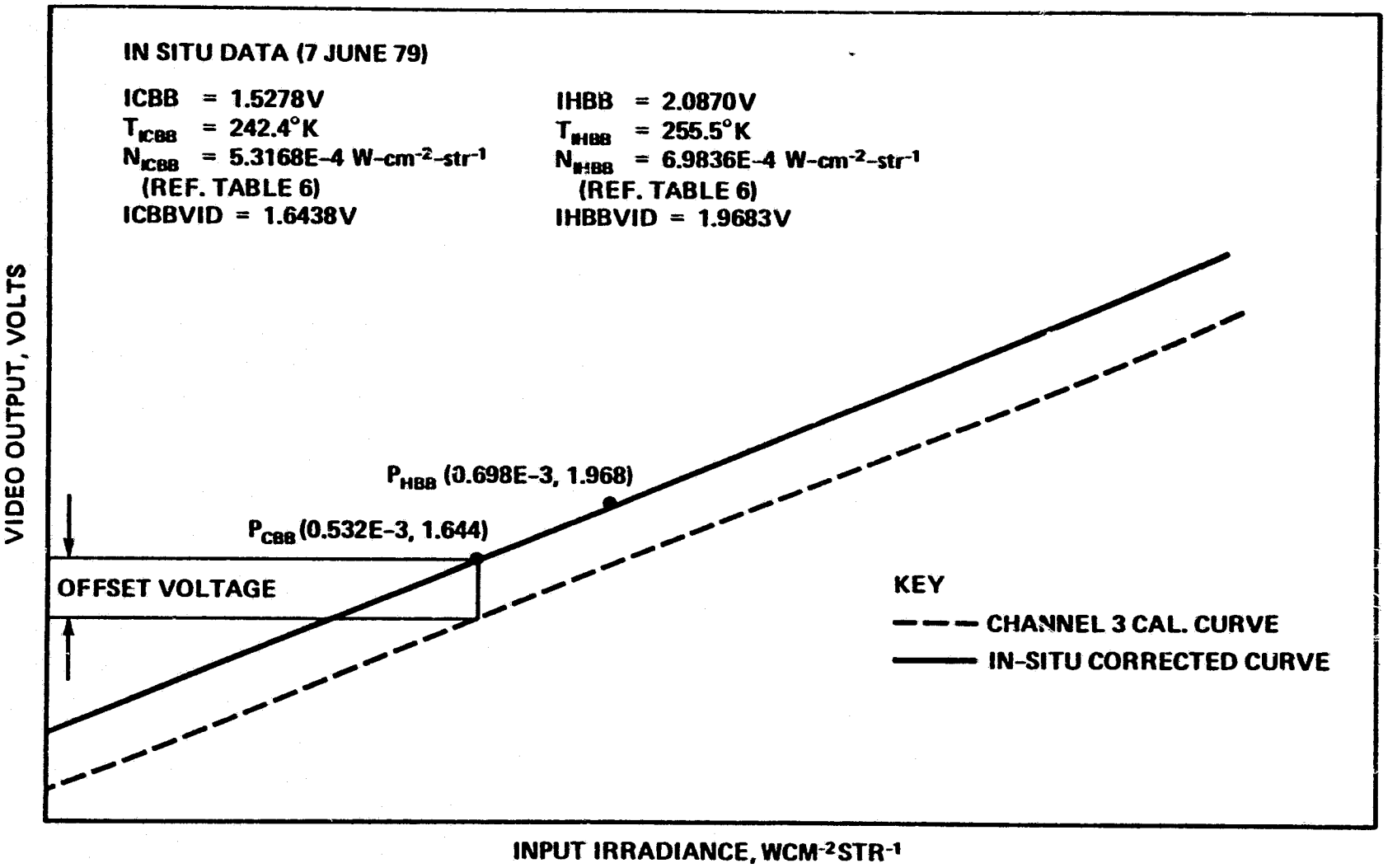

Figure 12. Flight Data Correction Schematic

REFERENCES

1. W. E. Shenk and R. J. Curran, Journal of Applied Meteorology, Vol. 12, No. 7, 1213 (1973).

2. R. F. Adler et al., Thunderstorm Top Structure Observed by Aircraft Overflights with an Infrared Radiometer. To be presented: 12th Severe Local Storms Conf., S. Antonio, TX (Jan. 1982).

3. K. S. Brown, Specification for Cloud Top Scanner, S-944-2, GSFC, Greenbelt, MD, June 1974.

4. W. L. Wolf, ed.: Handbook of Military Infrared Technology, Office of Naval Research, Dept. of the Navy, Wash., D.C., 1965, p. 735.

5. Remote Sensing Technology and Applications, Purdue University Laboratory for Application of Remote Sensing, p. 63, Business Office, CE Rm. 110, Stewart Center, Purdue University, W. Lafayette, IN, 47907, 1972.

6. Self Study Manual on Optical Radiation Measurements, Part I, p. 70, National Bureau of Standards, TN910-2, Feb. 1978.

7. IBID, p. 77.